PERMEATION OF WATER THROUGH CATION EXCHANGE MEMBRANES

N. LAKSHMINARAYANAIAH

From the Department of Pharmacology, School of Medicine, University of Pennsylvania Philadelphia, Pennsylvania 19104

ABSTRACT Water permeabilities as well as other membrane parameters, such as exchange capacity, water content, and specific conductance, have been measured for two cation exchange membranes in the H form. The conductance of membrane with low water content was less than that of the membrane with high water content. These data have been discussed in the light of an existing theory and found inadequate to explain the results in a quantitative way. Water permeability of the membranes subject to mechanical pressure was found to be higher than their isotopic water permeability, according to expectation. These data have been examined from the standpoint of thermodynamic and kinetic theories of water flow in membranes and used to estimate the average size of membrane pores.

INTRODUCTION

Ion exchange membranes are cross-linked, three-dimensional polymer networks containing a number of fixed ionogenic groups (electronegative in the case of cation exchange membranes), and a considerable quantity of water which is controlled by the degree of cross-linking of polymer chains present in the case of homogeneous membranes. In the case of heterogeneous membranes, particularly of the type of membranes formed by compression molding of a binder and powdered ion exchange material, the quantity of water present is determined by the ratio in which the binder and the ion exchange material are held together; the greater the proportion of binder, the less is the water content of the membrane (1). Many of the transport properties of the membranes, as for example electroosmosis, bulk, and diffusional water flows, reviewed recently (2), are controlled by these two membrane properties, viz. exchange capacity and water content.

The microstructure of the membranes has been determined by diffusion and exchange studies by Gärtner et al. (3), while Schurig and Schlögl (4) estimated the pore size distribution by measurement of diffusion coefficients of tagged counterions at temperatures below 0°C. Other investigators (5–7) studied water vapor adsorption and desorption to evaluate the average pore diameters of ion exchangers. In a recent paper, Kawabe et al. (8) have developed a complex equation relating the equivalent

conductance of the membrane in different ionic forms to the average radius of the membrane pores. This approach, as well as the others referred to above, is different from the classical approach normally used to derive an average value for the radius of the pores present in nonionic membranes. This classical method, based on the measurement of bulk flow of water through the capillaries of the membrane subject to the influence of a mechanical pressure gradient and developed by physiologists (9–11), does not seem to have been applied to ionic membranes to estimate the average size of their pores. This paper therefore presents the results of such a study for two cation exchange membranes.

MATERIALS AND METHODS

Cation Exchange Membranes

Cross-linked phenolsulfonic acid (PSA) membranes were prepared following the method already described (12). These membranes, according to Helfferich (13), may be considered homogeneous, although in operational behavior they are heterogeneous (14).

Polyethylene-styrene graft copolymer type AMF C-103 membranes containing sulfonic acid groups were supplied by American Machine and Foundry Company. These membranes, although dubbed homogeneous (15), are probably more heterogeneous functionally than PSA membranes.

Membranes were washed thoroughly with distilled water and converted to the H form by conditioning them in 1 N HCl. After the acid was decanted, they were rinsed several times with deionized water in which they were stored.

Water Content

Pieces of membrane were blotted with filter paper, placed in a weighing bottle, and weighed. They were then dried to constant weight in a vacuum desiccator at 60°C.

Ion Exchange Capacity

A known weight of membrane in the H form was equilibrated with stirring overnight in 1 N KCl. The acid released into the solution was estimated by titration with 0.1 N KOH.

Membrane Thickness and Resistance

The *H* form of the membrane, surface-dried between filter papers, was held in micrometer calipers for thickness measurement.

A cell of the type used by Kawabe et al. (8) was used for membrane resistance measurements.

Measurement of Bulk Flow of Water

A cell of the type shown in Fig. 1 *a* was used. Two pieces of industrial glass piping (I.D. 19 mm) formed the cross-member of an ⊔ cell. Fig. 1 *b* gives an exploded view of the assembly holding the membrane supported by a stainless steel mesh. Between the mesh and the membrane, filter paper was used to ensure complete wetting of the membrane surface on the low pressure side. The two half-cells (capacity, about 25 ml) were filled with deionized water and

immersed in a water thermostat maintained at 22° ± 0.1°C. The membrane assembly was covered with Plasticine clay to prevent direct contact of the membrane with the liquid in the thermostat. Mechanical pressure was applied to the side on which the membrane was in direct contact with water. Immediately on application of pressure, the liquid level on the low pressure side rose, indicating movement of the membrane. Sufficient time (about 1 hr) was allowed for this movement to stabilize itself. During this period, the whole assembly came to thermal equilibrium with the thermostatic liquid.

The flow of water under the influence of the applied pressure (exactly known as mm Hg on the manometer) was followed with time on a cathetometer. The area of the membrane exposed to the liquid under pressure was 2.84 cm².

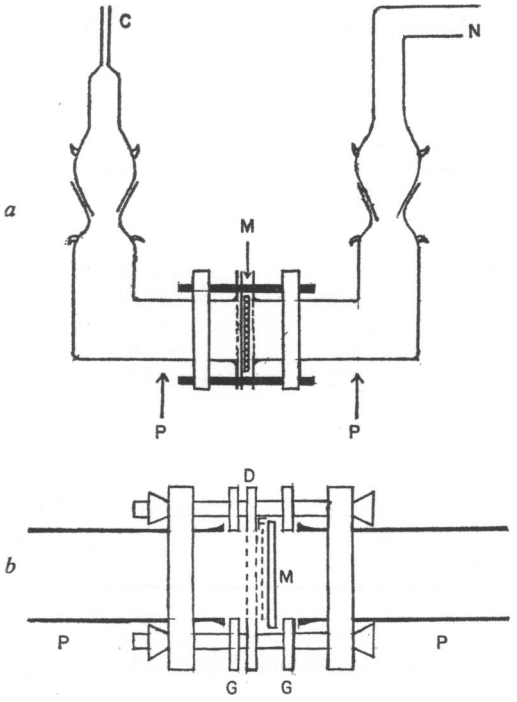

FIGURE 1 *a*, apparatus for measuring bulk flow of water. *C* is a precision bore capillary tubing. *P* is the two pieces of industrial glass piping holding the membrane (*M*). The tube (*N*) is connected to a nitrogen cylinder through a mercury manometer to record the applied pressure. *b*, exploded view of the water transport cell containing the membrane assembly. *P* is the two pieces of industial glass piping holding the membrane (*M*) between rubber gaskets (*G*). *D* is the Plexiglas disc containing the stainless steel mesh supporting the membrane. *F* is the filter paper held between *D* and *M*.

Movement of Tritiated Water

A cell similar to the one used in bulk flow measurements was used with minor modifications. The two half-cells had a capacity of approximately 200 ml. The membrane, surface-dried by blotting with filter paper, was clamped with or without support as required, and the liquid on either side was stirred using rotating magnets at high speed. Here also the "hot" solution, i.e. water containing 1 μc/ml tritiated water (THO), was in direct contact with the 2.84 cm² membrane surface.

Exactly 150 ml of deionized water were added to the "cold" side, and precisely the same volume of THO to the "hot" side. When nearly 75 ml of THO were transferred, a stopwatch was started. At regular intervals of time, an aliquot of exactly 1 ml of liquid on the "cold" side was taken for counting. This loss in volume each time 1 ml was taken out was compensated by adding 1 ml of deionized water.

The aliquot taken for counting was transferred into a polyethylene vial (capacity, about 25 ml) into which 20 ml of Bray's solution (16) were added and mixed. The samples were counted in a Packard Tri-Carb liquid scintillation counter. All these experiments were carried out in an air-conditioned room at 22°C.

RESULTS

Different membrane parameters with standard errors of the mean determined for the two membranes are given in Table I. The water content and the exchange capacity of PSA membranes are considerably higher than those of AMF membranes, and as a result the former conduct more efficiently than the latter. Equating roughly the amount of water in the membrane to the void space, it is seen that PSA membranes are more porous than AMF membranes.

TABLE I
MEMBRANE CHARACTERISTICS IN THE H FORM

Membrane	PSA	AMF C-103
Thickness (μ)	292 ± 10*	152 ± 5*
Water content (g/g wet membrane)	0.59 ± 0.04	0.21 ± 0.01
Density (g/ml)	1.16 ± 0.04	1.08 ± 0.04
Volume fraction of resin, V_r	0.33	0.77
Exchange capacity (eq/liter)	1.39 ± 0.04	0.86 ± 0.02
Specific conductance in 0.1 N HCl, $k(\text{ohm}^{-1}\cdot\text{cm}^{-1}) \times 10^3$	92 ± 2	18 ± 0.5
Diffusion coefficient, $\bar{D}_{\text{THO}}(\text{cm}^2\cdot\text{sec}^{-1}) \times 10^7$		
Membrane supported	3.9 ± 0.2	1.2 ± 0.1
Unsupported	9.4 ± 0.5	2.1 ± 0.1
$\bar{D}_{\text{THO}} \times 10^7$ [calculated using equation (12)]	62	4.1

* One standard error of the mean.

Flow of Water under Mechanical Pressure (Volume or Bulk Flow)

In Figs. 2 and 3 are given the results of volume flow as a function of applied pressure for the PSA and AMF membranes, respectively. The bulk flow J_v (milliliters per min) is linearly proportional to applied pressure ΔP (cm Hg) according to the equation

$$J_v = L_p \cdot \Delta P, \tag{1}$$

where L_p is the filtration or hydraulic permeability coefficient (2). The values of L_p for the two membranes, expressed as $\text{cm}^5/(\text{dyne}\cdot\text{sec})$, are given in Table II (ΔP expressed as dynes per square centimeter). The values of L_p are in keeping with the water content of membranes; the larger the water content, the larger the value of L_p. Experiments in this series were done both with and without stirring, and the values of L_p realized were not significantly different.

Diffusional Flow of Tritiated Water

In Fig. 4 a plot of radioactivity (counts per minute) accumulating on the "cold" side against time is given. As the membrane became equilibrated with the "hot" solution, a steady state of flux of THO across the membrane was reached. The hold-up time was determined by extending the steady state straight line to cut the

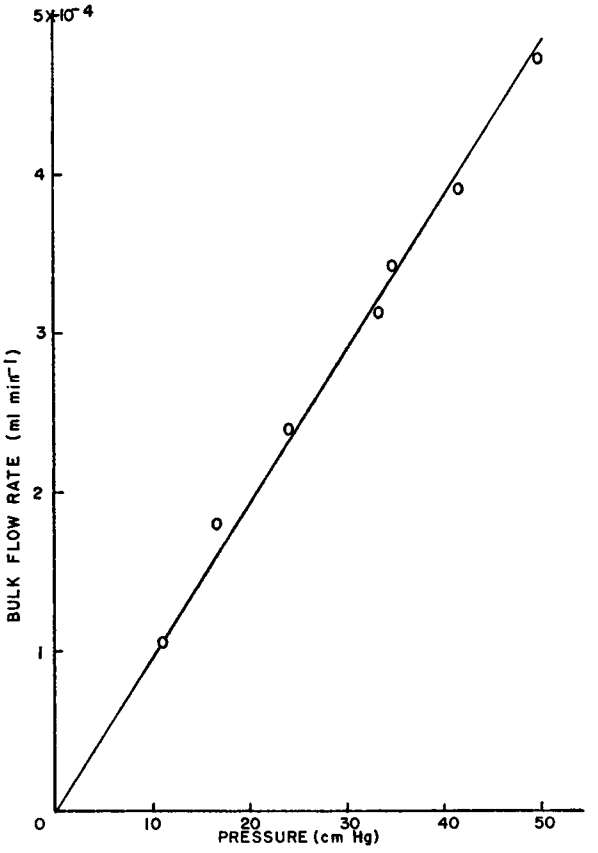

FIGURE 2 A plot of bulk flow rate of water through a supported PSA membrane against applied pressure.

time axis (17, 18). This time was related to the diffusion coefficient of the species moving through the membrane by the equation (17–19)

$$\bar{D} = \frac{(\Delta X)^2}{6t}, \tag{2}$$

where $\bar{D}$ is the diffusion coefficient of the species ($cm^2\ sec^{-1}$), ΔX is the thickness of the membrane (centimeters), and t is the hold-up time (seconds).

This equation has been used by Wright (19) to derive the self diffusion coefficients of Na and Br ions in horn keratin. Similarly, equation (2) has been used in this study to derive $\bar{D}$ values for THO in PSA and AMF membranes. The $\bar{D}_{THO}$ values so derived for both supported and unsupported membranes using the same value of ΔX are given in Table I.

The values of $\bar{D}_{THO}$ for the supported membranes are lower than those for the unsupported membranes. This may be attributed to the presence of filter paper and different unstirred layers of liquid between the membrane, the filter paper, and the support. These thus add thickness to the membrane and thereby increase the hold-up time, giving a low value for $\bar{D}_{THO}$.

Making reasonable assumptions about the diffusion coefficient of THO in these intervening liquid layers and their thickness, a value for $\bar{D}_{THO}$ for the supported

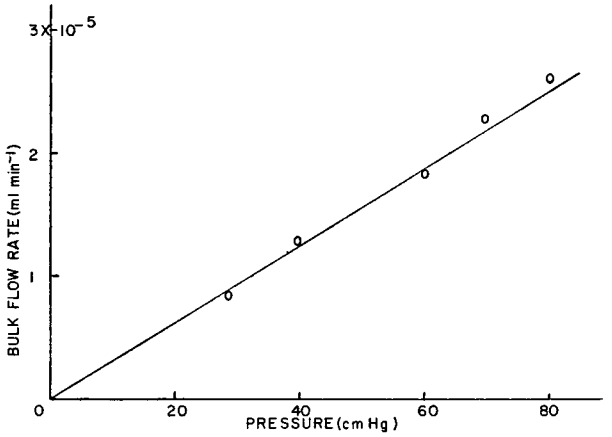

FIGURE 3 A plot of bulk flow rate of water through a supported AMF membrane against applied pressure.

membrane may be derived using an experimentally determined value of $\bar{D}_{THO}$ for the unsupported membrane. According to the analysis given by Kedem and Katchalsky (20), the permeability P of a species i moving through a composite membrane consisting of an array of j elements in series is given by

$$\frac{1}{P} = \sum_j \frac{1}{P_j}, \tag{3}$$

where P_j is the permeability of i through the jth element. For our particular case, Equation (3) becomes

$$\frac{1}{P_s} = \frac{1}{P_u} + \frac{1}{P_p} + \frac{1}{P_w}, \tag{4}$$

where P_s, P_u, P_p, and P_w are the permeabilities of THO through the supported

membrane, unsupported membrane, filter paper, and different water layers, respectively. Since permeability P is related to diffusion coefficient $\bar{D}$ by (21)

$$\bar{D} = RT\, P\Delta X \tag{5}$$

TABLE II
WATER PERMEABILITY THROUGH MEMBRANES

Line	Membrane	PSA	AMF C-103
1	Permeability coefficient: filtration, L_p (cm^6/dyne·sec) $\times 10^{12}$		
	Membrane supported	12.4 ± 1.0	0.33 ± 0.04
	Unsupported	40.0 ± 3.9	0.59 ± 0.04
2	Diffusion, $D_w A_w/\Delta X$ (cm^3·sec^{-1}) $\times 10^5$		
	Supported	18.1 ± 1.0	6.62 ± 0.51
	Unsupported	49.0 ± 2.0	10.3 ± 0.5
3	Total flow due to ΔP $(L_p/18) \times 10^{15}$ (moles sec^{-1}/dyne·cm^{-2})		
	Supported	689	18.3
	Unsupported	2222	32.8
4	$(dn/dt)_{THO}$, diffusional flow [equation (8)] (mole sec^{-1}/dyne·cm^{-2}) $\times 10^{15}$		
	Supported	7.4	2.7
	Unsupported	20	4.2
5	Flux ratio (diffusion/total)		
	Supported	1/93	1/7
	Unsupported	1/111	1/8
6	K_s (cm^2) $\times 10^{16}$		
	Supported	11.9	0.16
	Unsupported	38.4	0.28
7	D (cm^2·sec^{-1}) $\times 10^5$		
	Supported	26.5	1.20
	Unsupported	85.5	2.03
8	$A_w/\Delta X$ (cm)		
	Supported	7.42	2.72
	Unsupported	20.1	4.2
9	r (A) [equation (16)]		
	Supported	34.5	9.3
	Unsupported	37.7	10.0
10	Fractional pore area (A_w/A)	0.207	0.023
11	No. of pores per unit area	6×10^{11}	13×10^{11}

Equation (4) becomes

$$\frac{(\Delta X)_s}{\bar{D}_s} = \frac{(\Delta X)_u}{\bar{D}_u} + \frac{(\Delta X)_p}{\bar{D}_p} + \frac{(\Delta X)_w}{\bar{D}_w}. \tag{6}$$

The values of $(\Delta X)_u$, $\bar{D}_u$, and $(\Delta X)_p$ are 0.0292 cm, 9.4×10^{-7} cm^2 sec^{-1}, and 0.02 cm, respectively. The value of $\bar{D}_p$ will be less than $\bar{D}_w$. Assigning a value of

10^{-6} for $\bar{D}_p$, the first two terms of the right-hand side of equation (6) amount to 0.51×10^5 cm^{-1} sec.

It is very difficult to estimate $(\Delta X)_w$ as there are many unstirred layers. It is realistic to say that in the experimental setup used in this study, there is "trapped water" between membrane and filter paper, and between filter paper and membrane support. It is also not unreasonable to expect a significant layer, or probably a film, of liquid to exist on the outer edge of the stainless mesh support on the "cold" side. Stewart and Graydon (22) estimated, using very low shaking rates (30 oscillations/min), the thickness of the liquid layer to be 330 μ. The liquid layers in our system are so situated that they are likely to remain undisturbed by the high rates of stirring employed in the bulk liquid. Assuming a maximum of four stagnant water layers (one at membrane face, two at the two faces of the filter paper, and one at the support), each of thickness 0.033 cm, $(\Delta X)_w$ will be 0.132 cm. Using 2.44×10^{-5} as the value for $\bar{D}_w$, the value for the diffusion of THO in Water (23), the contribution of the last term in equation (6) will be 0.054×10^5. As $(\Delta X)_s$ is 0.0292 cm, the value used in equation (2) to calculate $\bar{D}_{THO}$ for the supported membrane, $\bar{D}_s$ will come out to be 5.2×10^{-7} cm^2 sec^{-1}. To realize the observed value of 3.9×10^{-7} for $\bar{D}_s$, a value of about 0.6 cm must be assigned to $(\Delta X)_w$. This value is too high to be true. It becomes even more unrealistic if a value higher than 10^{-6} cm^2 sec^{-1} is used for $\bar{D}_p$. Thus it is thought that the value of $\bar{D}_w$ used is probably too high.

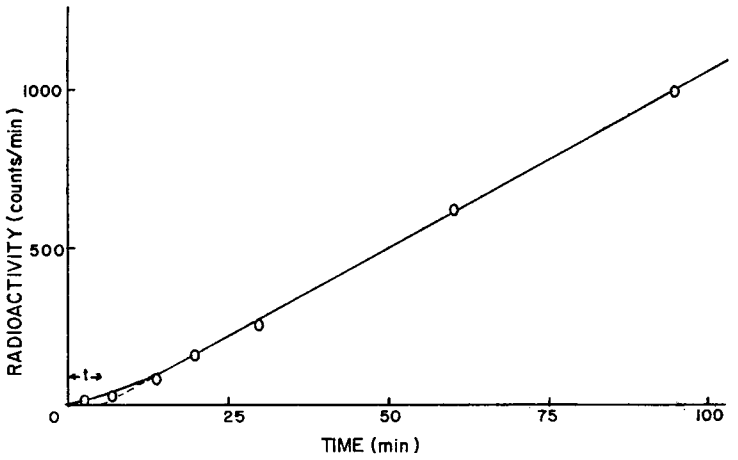

FIGURE 4 Quantity of radioactivity accumulating on the "cold" side of a supported AMF membrane, plotted as a function of time.

The water layers existing at the membrane and filter paper interfaces are likely to possess properties different from those of bulk water. Water dipoles existing at the interfacial regions will have lost some of their translational degrees of freedom and consequently will offer greater resistance to flow of THO. $\bar{D}_w$ will be probably of the

order of 10^{-6} cm^2 sec^{-1}. If a value of 0.1 cm is used for $(\Delta X)_w$ and a reasonable value of 4×10^{-6} for $\bar{D}_w$, $\bar{D}_s$ will have a value of 3.8×10^{-7} cm^2 sec^{-1}, agreeing with the observed value.

Similar calculations made for AMF membrane gave a value of 1.3×10^{-7} cm^2 sec^{-1} for $\bar{D}_s$, again in agreement with the observed value.

In view of these calculations, it becomes apparent that "trapped water" existing in the region of interfaces offers considerable resistance to diffusion and thereby lowers the value for $\bar{D}_{\text{THO}}$ for the supported membrane. The increase in hold-up time in these cases seems, therefore, to be due more to the slowness of diffusion than to the increase in thickness of the barrier.

The values of $\bar{D}_{\text{THO}}$ for AMF membranes are lower than the corresponding values for PSA membranes, as expected, because of their lower water content. The hold-up times for the supported and unsupported membranes were 5 and 3 min, respectively, in contrast to 6 and 2.5 min realized for the PSA membranes. This seems to indicate that diffusion is controlled more by the membrane and less by the stagnant liquid film in the case of the AMF membrane than it is in the case of the PSA membrane (see discussion on bilayer membrane).

The values of $\bar{D}_{\text{THO}}$ derived in this manner gave little information about the porosity or the average radius of pores of the membrane. In order to determine this, the approach made by physiologists (9, 10, 24–28) was adopted.

Fick's law for diffusion of THO may be written according to Mauro (29) as

$$\frac{dn}{dt} = \frac{D_w A_w}{RT} C \frac{d\mu}{dX}, \tag{7}$$

where dn/dt is the rate of transport of n (i.e. THO). Change in chemical potential, $d\mu$, $= \bar{V}\, dP$, and $C\bar{V} = 1$. $\bar{V}$ is the partial molar volume, C the concentration, and dP the change in pressure. D_w is the diffusion coefficient of THO in water contained in the pore volume of area A_w and pore length dX which n should traverse. R and T have their usual significance.

Making the substitutions and writing dP/dX as $\Delta P/\Delta X$, since dP/dX is a constant, equation (7) becomes

$$\frac{dn}{dt} = \frac{D_w A_w}{\Delta X} \frac{\Delta P}{RT}. \tag{8}$$

Equating ΔP to osmotic pressure, i.e. $RT\Delta C_{\text{THO}}$, we obtain

$$\left(\frac{dn}{dt}\right)_{\text{THO}} = \frac{D_w A_w}{X} \Delta C_{\text{THO}}. \tag{9}$$

Equation (9) was integrated originally by Northrop and Anson (30) and recently by Robbins and Mauro (27). Dainty and House (31) have given a general integrated

equation in the form

$$\frac{D_w A_w}{\Delta X} = \frac{2.303 V_1 V_2}{(V_1 + V_2)\Delta t} \log \frac{C' V_1 + C'' V_2 - C''_{t_0}(V_1 + V_2)}{C' V_1 + C'' V_2 - C''_{t_0+\Delta t}(V_1 + V_2)}, \tag{10}$$

where V_1 and V_2 are the volumes of compartments 1 ("cold" side) and 2 ("hot" side). C' and C'' are the initial concentration (taken as counting rate per milliliter) of tritium in compartments 1 and 2, i.e. at $t = 0$. C''_{t_0} and $C''_{t_0+\Delta t}$ are the concentrations in compartment 2 at time $t = t_0$ and $t = t_0 + \Delta t$, respectively. Δt therefore is the time elapsing between samplings, in seconds. t_0 is not zero time but the time at which the initial sample required for evaluation of $D_w A_w/\Delta X$ is withdrawn.

As we have used equal volumes in this work, equation (10) reduces to the form given by Robbins and Mauro (27), and becomes further simplified for the conditions of our experiments, viz. $C' = 0$, to

$$\frac{D_w A_w}{\Delta X} = \frac{1.15 V}{\Delta t} \log \frac{C'' - 2C''_{t_0}}{C'' - 2C''_{t_0+\Delta t}}. \tag{11}$$

A plot of log $[C''/(C'' - 2C''_{\Delta t})]$ (where $C''_{\Delta t}$ is $C''_{t_0+\Delta t}$ when $t_0 = 0$) against time (Fig. 5) gives a straight line according to equation (11). However, in this work $D_w A_w/\Delta X$ was evaluated numerically, and values for $A_w/\Delta X$ given in Table II were calculated using the literature value for D_w[D_w(THO) = 2.44×10^{-5} cm^2 sec^{-1}] (23).

DISCUSSION

Diffusion of Tritium and Conductance of the Membranes

The values of diffusion coefficients given in Table I for the two membranes are in keeping with the values obtained by other investigators (32) using more exact methods. Because high rates of stirring were used, it is reasonable to assume that the gradient of chemical potential for THO acted across the thickness of the membrane (unsupported) and that the $\bar{D}_{\mathrm{THO}}$ values refer to the membrane phase. These values are lower than the self-diffusion of THO (23) by a factor of nearly 100. Mackay and Meares (33), using Zeokarb 315 discs, which are chemically similar to PSA membranes, studied the self-diffusion of Na ions and found the self-diffusion coefficient in the membrane to be lower than that in the aqueous solution. This lowering was attributed to the hindrance which the membrane polymer matrix offered to the movement of ions. This in turn increased the tortuosity of the diffusion path. Meares et al. (33–35) have considered this factor in great detail and expressed the diffusion in the membrane by the equation

$$\bar{D}_{\mathrm{THO}} = D_{\mathrm{THO}} \left(\frac{1 - V_r}{1 + V_r}\right)^2. \tag{12}$$

The values for the volume fraction (V_r) of the resin for our membranes and $\bar{D}_{THO}$ values calculated according to equation (12) are given in Table I. As found by other workers (36–38), the agreement between measured and calculated $\bar{D}_{THO}$ values is poor, although the disagreement is less for the AMF membranes, which have less water. Consequently, it is inferred either that the membrane matrix offers greater hindrance to diffusion than the simple Meares function would indicate or that other mechanisms of transport, like diffusion along polymer chains which may be continuous or discontinuous, are involved.

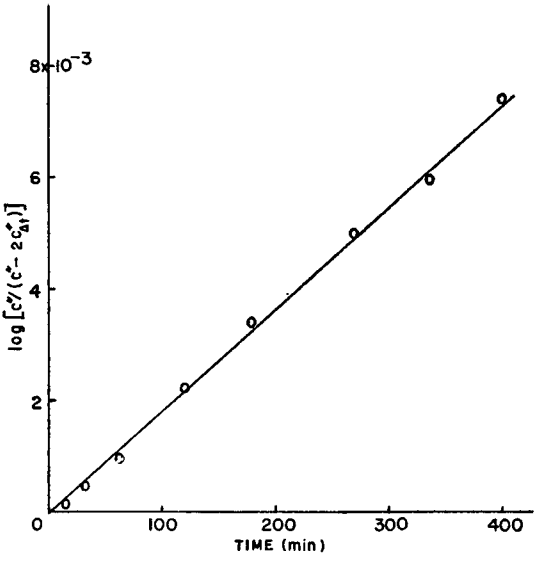

FIGURE 5 A plot of the function log $[C^\circ/(C^\circ - 2C^\circ_{\Delta t})]$ against time.

Experimentally determined $\bar{D}_{THO}$ values may be used to calculate the equivalent conductance $\bar{\lambda}$ of the H form membrane, assuming applicability of the Nernst-Einstein relation (39), viz.

$$\bar{D}_{THO} = \frac{RT}{F^2}\,\bar{\lambda}_{THO}, \tag{13}$$

to our membrane system. $\bar{\lambda}_{THO}$ ($cm^2\Omega^{-1}$ eq^{-1}) values obtained are 3.6 and 0.8 for PSA and AMF membranes (unsupported), respectively. However, the values obtained by direct measurement of membrane resistance (in 0.1 N HCl) are 66.2 and 20.9. These discrepancies between measured $\bar{\lambda}$ (membrane in the H form) and $\bar{\lambda}_{THO}$ derived from equation (13) are very large. Small differences between such values have been observed by a number of workers (36–40). These differences seem to arise from the different conditions under which the mobile ions of the membrane phase are made to migrate. When counterions present in the charged membrane,

i.e. containing a number of ionized groups fixed to the membrane matrix, move under the influence of an electric field, they cause an electroosmotic flow of water in the same direction but at a lower linear velocity (41). In relation to the membrane matrix, counterions move faster than they otherwise would if water were standing still (akin to swimming with the tide). Consequently, measured conductance is higher than the conductance corresponding to a state in which water is at rest, a situation that prevails in self-diffusion experiments. Therefore, the difference between the two values has been attributed to electroosmosis (36–40). But in the case of our results, the differences are due, besides electroosmosis, to (*a*) the presence of excess H^+ counterions and Cl^- coions in the membrane phase in direct conductance measurements and (*b*) the presence of tritium, which is less mobile than H^+, and the absence of HCl in the membrane phase in self-diffusion measurements.

Nature of Water Flow Through the Membranes

The nature of water flux occurring across a membrane subjected to a mechanical pressure difference is difficult to assess on ordinary grounds. Both Ticknor (42) and Mauro (29) have analyzed this problem from the kinetic and the thermodynamic points of view, respectively. Ticknor found that the type of flow depended on the sizes of the permeating species and of the capillaries of the membrane, and on the degree of bonding the mobile species had for the membrane material. On theoretical grounds he estimated that the rates of both diffusional and viscous flows would be equal when the pore radius of the membrane capillaries was nearly twice the radius of the permeating molecules. It was surmised that when the pore radius was larger than the radius of the permeating molecule the flow would be laminar in nature, and that when they became nearly equal, the flow would be diffusional in character. A statistical treatment of diffusion in such narrow pores, where overtaking by molecules is not permitted, has been recently given by Longuet-Higgins and Austin (43).

Analysis by Robbins and Mauro (27) has shown that the solvent flow by osmosis is made up of both viscous and diffusional components. For most barriers, it was shown that the predominant component was the viscous flow. Application of this analysis to our experimental results is shown in Table II. The results of line 4 were obtained from equation (8) for the case $\Delta P = 1$. It is obvious from the results given in line 5 that the viscous flux is larger than the diffusional flux by a factor of 100 in PSA and 7 in AMF membranes. Thus, as the membrane pores became smaller, a larger portion of the viscous flux was due to diffusion.

According to the analysis given by Ticknor (42), the filtration permeability coefficient K_s (cm^2) is given by

$$K_s = \frac{Vl\eta}{tA\Delta P} = \frac{L_p l\eta}{A}, \tag{14}$$

where l is the thickness of membrane of area A and η is the viscosity of the pore

liquid. A diffusion coefficient was computed from the K_s values using the relation

$$D = \frac{RTK_s}{\epsilon \bar{V} \eta} \tag{15}$$

(ϵ = fractional void volume). Values of K_s and D calculated for our membranes are also given in Table II. The D values, according to theory, should approach the self-diffusion coefficient of water ($\sim 2 \times 10^{-5}$) as the nature of flow through the membrane changes from viscous to diffusional. Accordingly, the D values indicate that the flow in the PSA membrane is mostly laminar, whereas that in the AMF membrane is mostly diffusional. Qualitatively, this analysis agrees with that given above, where a direct measurement of diffusion of THO was carried out. A D value in the AMF membrane of 2×10^{-5} cm^2 sec^{-1} is in quantitative agreement with Ticknor's theory. This agreement should be considered fortuitous in view of the fact that the theory is idealized and does not take into account the frictional factors involved in the transport of water through the membrane.

In the context of this discussion, the experimental finding that the two water permeability coefficients, viz. osmotic and isotopic, derived for the phospholipid bilayer membranes by two groups of workers (44–48) are different is attributable to the basic difference in the mechanism of water flux under conditions of volume flow and isotopic exchange flow. However, Hanai et al. (45) attributed this difference to the presence of stagnant liquid layers at the two faces of the membrane in isotopic flux measurements. Huang and Thompson (47), on the other hand, have rejected this explanation. The fact that the bilayers are permeable to water indicates that the phospholipid matrix has "space vacancy," the nature of which may be either static (i.e. a pore) or dynamic (thermal fluctuations of hydrocarbon chains), allowing water to go through. Further, the resistance of the membrane being of the order of 10^9 ohms·cm^2, the diffusion transport across it would be mostly controlled by the membrane and very little by the stagnant liquid films. In very porous membranes of the type studied by Hanai et al. (45), viz. cellophane and glass mesh, whose resistances are not that high, stagnant layers would control diffusion to a larger extent (31, 49). As a result, to attribute all the difference between the two permeability coefficients to stagnant liquid layers alone becomes less tenable.

Converting the permeability coefficients obtained by Huang and Thompson (47) for the phosphatidylcholine bilayer (CH-21) into the units employed in this paper, the values obtained for L_p and $D_w A_w / \Delta X$ are 8.5×10^{-15} (membrane area, 6.99×10^{-3} cm^2) and 2.53×10^{-6}, respectively. According to Mauro's analysis, the ratio diffusional flux/total flux is 1/4.7.

Determination of Equivalent Pore Radius

In a recent review article (2), the applicability of different permeability equations which have been used by different workers to derive the average radius of membrane

pores was discussed. It was concluded that the equation

$$r = \sqrt{\frac{8\eta L_p}{(A_w/\Delta X)}} \tag{16}$$

(r = radius of pores) gave reliable values for r. However, it must be remarked that, in the light of the results of this study, the values of r derived for various membranes by Renkin (24) and Durbin (28) are underestimated, as in their diffusion studies to derive $A_w/\Delta X$ they did not use any support for the membrane, whereas to measure L_p support was used. Unsupported membranes always gave high flow rates (see Table II). Provided L_p and $A_w/\Delta X$ are measured under identical conditions, values derived for r from equation (16) should not be significantly different. Such is the case, as is evident from the values of r derived for the two membranes and shown in Table II.

Calculation of r using equation (16) does not take into account (9, 10, 24) (*a*) steric hindrance at the pore entrance or (*b*) frictional resistance with the pores felt by the permeating molecules. Paganelli and Solomon (25, 50), taking these factors into account, have given a simple equation,

$$r = -a + \sqrt{2a^2 + \frac{8\eta L_p}{(A_w/\Delta X)}}, \tag{17}$$

where a is the radius of the permeating molecule. Using a = 1.97 A in equation (17), values of 32.6 and 7.6 A are obtained for the PSA and AMF membranes, respectively. As the value of r for the PSA membrane is not very much affected, the factors mentioned above are ineffective in membranes whose pore size is large compared to the size of the permeating molecule, whereas they do have an effect when the pore size is of molecular dimensions.

Kawabe et al. (8), employing the same AMF C-103 membranes as used in this study but a different experimental technique and computer calculations using a complex but empirical equation, have evaluated the pore size to be 5.4 A. The difference between this value and the 7.5 A derived in this study should be considered insignificant in the context of (*a*) the divergent experimental techniques used in the two studies and (*b*) the number of different assumptions on which the two methods are based.

From the values of $A_w/\Delta X$ (see Table II) and r worked out for the unsupported membranes, the fractional pore areas, i.e. A_w/A, and the number of pores present in 1 cm^2 of the membrane surface were calculated. The values realized are also shown in Table II.

Longuet-Higgins and Austin (43), in their paper, illustrated the application of the solvent flux equation derived from statistical consideration of the kinetics of osmotic transport across membranes to calculate the number of pores per unit area of plasma membrane. Their equation is applicable to membranes containing pores of molecu-

lar dimensions such that permeating molecules cannot overtake. Assuming that relaxation of this condition is permitted in the case of the AMF membrane, the number of pores per unit area of membrane was calculated. The value was 98×10^{11}. The osmotic (i.e. L_p) and diffusional fluxes measured separately are in the proportion 8:1 (Table II). For this proportion to be equal, the number of pores would be 98/8 or 12×10^{11}, which agrees with the value realized from *THO* flux measurements. Provided that the different fluxes are properly recognized, equations (7)–(9) derived from thermodynamic considerations are equivalent to the statistically derived equation of Longuet-Higgins and Austin.

The work was supported in part by grants GB-4452 from the National Science Foundation and NB-03321 from the National Institute of Neurological Diseases and Blindness.

Received for publication 19 January 1967.

REFERENCES

1. HALE, D. K., and D. J. MCCAULEY. 1961. *Trans. Faraday Soc.* **57**:135.
2. LAKSHMINARAYANAIAH, N. 1965. *Chem. Rev.* **65**:491.
3. GÄRTNER, K., R. GRIESZBACH, and E. ANTON. 1961. *Kolloid. Z.* **175**:123.
4. SCHURIG, H., and R. SCHLÖGL. 1959. *Angew. Chem.* **71**:466.
5. BLASIUS, E., H. PITTACK, and N. NEGWER. 1956. *Angew. Chem.* **68**:671.
6. BLASIUS, E., and H. PITTACK. 1959. *Angew. Chem.* **71**:445.
7. BLASIUS, E., and W. HEIN. 1961. *Angew. Chem.* **73**:676.
8. KAWABE, K., H. JACOBSON, I. F. MILLER, and H. P. GREGOR. 1966. *J. Colloid Sci.* **21**:79.
9. PAPPENHEIMER, J. R., E. M. RENKIN, and L. M. BORRERO. 1951. *Am. J. Physiol.* **167**:13.
10. PAPPENHEIMER, J. R. 1953. *Physiol. Rev.* **33**:387.
11. KOEFOED-JOHNSEN, V., and H. H. USSING. 1953. *Acta Physiol. Scand.* **28**:60.
12. LAKSHMINARAYANAIAH, N., and V. SUBRAHMANYAN. 1964. *J. Polymer Sci.* **A2**:4491.
13. HELFFERICH, F. 1962. Ion Exchange. McGraw-Hill Book Company, Inc., New York. 61.
14. SUBRAHMANYAN, V. 1961. Doctorate Thesis. Madras University, India.
15. SHAFFER, L. H. 1966. *J. Electrochem. Soc.* **113**:1.
16. BRAY, G. A. 1960. *Anal. Biochem.* **1**:279.
17. BARRER, R. M. 1941. Diffusion in and through Solids. Cambridge University Press, New York. 14.
18. HELFFERICH, F. 1962. Ion Exchange. McGraw-Hill Book Company, Inc., New York. 352.
19. WRIGHT, M. L. 1953. *Trans. Faraday Soc.* **49**:95.
20. KEDEM, O., and A. KATCHALSKY. 1963. *Trans. Faraday Soc.* **59**:1945.
21. GINZBURG, B. Z., and A. KATCHALSKY. 1963. *J. Gen. Physiol.* **47**:403.
22. STEWART, R. J., and W. F. GRAYDON. 1956. *J. Phys. Chem.* **60**:750.
23. WANG, J. H., C. V. ROBINSON, and I. S. EDELMAN. 1953. *J. Am. Chem. Soc.* **75**:466.
24. RENKIN, E. M. 1954. *J. Gen. Physiol.* **38**:225.
25. PAGANELLI, C. V., and A. K. SOLOMON. 1958. *J. Gen. Physiol.* **41**:259.
26. NEVIS, A. H. 1958. *J. Gen. Physiol.* **41**:927.
27. ROBBINS, E., and A. MAURO. 1960. *J. Gen. Physiol.* **43**:523.
28. DURBIN, R. P. 1960. *J. Gen. Physiol.* **44**:315.
29. MAURO, A. 1957. *Science.* **126**:252; 1960. *Circulation.* **21**:845.
30. NORTHROP, J. H., and M. L. ANSON. 1929. *J. Gen. Physiol.* **12**:543.
31. DAINTY, J., and C. R. HOUSE. 1966. *J. Physiol., (London).* **185**:172.
32. LAKSHMINARAYANAIAH, N. 1965. *Chem. Rev.* **65**:501.
33. MACKAY, D., and P. MEARES. 1959. *Trans. Faraday Soc.* **55**:1221.
34. MACKIE, J. S., and P. MEARES. 1955. *Proc. Roy. Soc. (London), Ser. A.* **232**:498, 510.

35. MEARES, P. 1956. *J. Polymer Sci.* **20:** 507; 1958. *J. Chim. Phys.* **55:**273.
36. DESPIĆ, A., and G. J. HILLS. 1957. *Trans. Faraday Soc.* **53:**1262.
37. JAKUBOVIC, A. O., G. J. HILLS, and J. A. KITCHENER. 1958. *J. Chim. Phys.* **55:**263; 1959. *Trans. Faraday Soc.* **55:**1570.
38. LAGOS, A. E., and J. A. KITCHENER. 1960. *Trans. Faraday Soc.* **56:**1245.
39. SPIEGLER, K. S., and C. D. CORYELL. 1953. *J. Phys. Chem.* **57:**687.
40. DESPIĆ, A., and G. J. HILLS. 1956. *Discussions Faraday Soc.* **21:**150.
41. SCHMID, G. 1952. *Z. Elektrochem.* **56:**181.
42. TICKNOR, L. B. 1958. *J. Phys. Chem.* **62:**1483.
43. LONGUET-HIGGINS, H. C., and G. AUSTIN. 1966. *Biophys. J.* **6:**217.
44. HANAI, T., D. A. HAYDON, and J. L. TAYLOR. 1965. *J. Gen. Physiol.* **48**(Suppl.):59.
45. HANAI, T., D. A. HAYDON, and W. R. REDWOOD. 1966. *Ann. N.Y. Acad. Sci.* **137:**731.
46. THOMPSON, T. E. 1964. *In* Cellular Membranes in Development. M. Locke, editor. Academic Press, Inc., New York. 83.
47. HUANG, C., and T. E. THOMPSON. 1966. *J. Mol. Biol.* **15:**539.
48. THOMPSON, T. E., and C. HUANG. 1966. *Ann. N.Y. Acad. Sci.* **137:**740.
49. DAINTY, J., and C. R. HOUSE. 1966. *J. Physiol., (London).* **182:**66.
50. DICK, D. A. T. 1966. Cell Water. Butterworth, Washington, D.C. 106.